Quasiparticle effective mass for the two- and three-dimensional electron gas

Andrey Krakovsky
Department of Physics, New York University, New York, New York 10003

Jerome K. Percus
Courant Institute of Mathematical Sciences and Department of Physics, New York University, New York, New York 10003

(Received 16 August 1995; revised manuscript received 7 November 1995)

We calculate the quasiparticle effective mass for the electron gas in two and three dimensions in the metallic region. We employ the single-particle scattering potential coming from the Sjölander-Stott theory and enforce the Friedel sum rule by adjusting the effective electron mass in a scattering calculation. In three dimensions (3D) our effective mass is a monotonically decreasing function of r_s throughout the whole metallic domain, as implied by the most recent numerical results. In two dimensions (2D) we obtain reasonable agreement with the experimental data, as well as with other calculations based on the Fermi-liquid theory. We also present results of a variety of different treatments for the effective mass in 2D and 3D.

I. INTRODUCTION

The evaluation of the Fermi-surface parameters has been a cornerstone of the Fermi-liquid theory since its early years. Precise knowledge of these parameters for an electron gas, especially in the metallic domain, is not only a fundamental problem, but is also extremely important for physical applications. At present, there is some controversy about the three-dimensional (3D) results at metallic and overmetallic densities. The two-dimensional results are also of significant importance due to the recent nonvanishing interest in the 2D physics stimulated by high-T_c superconductivity, the fractional quantum Hall effect, as well as the development of 2D electronic devices.

As is well known from textbooks, quasiparticle excitations can be characterized by the renormalization constant $Z(k_F)$, which is related to the residue of the Green's function at the Fermi surface, and the quasiparticle effective mass m^*. In a simple-minded physical picture, $1-Z(k_F)$ and $1-m^*/m$ both measure the amount of the many-body effects in the electron gas. In this paper we will be concerned with the effective (renormalized) electron mass. We will use the effective potential coming from the Sjölander-Stott theory,[1] and find the effective electron mass by adjusting the effective electron mass in a scattering calculation, so that the Friedel sum rule is satisfied. Our approach is ''hydrodynamic'' in a sense that it does not explicitly employ the microscopics of the Fermi liquid, however, it requires the ''correct'' static linear response function as an empirical input. Thus, the Fermi-liquid character of the electron gas will come in indirectly through the linear response that we use in a parametrized form.

Below we will outline the GW format, which is a basis for the majority of calculations of the Fermi-surface parameters. We will compare results of different approximation schemes with ours. For both 2D and 3D our results are in a reasonable agreement with the most recent calculations based on the Fermi-liquid theory, as well as experimental data.

II. EFFECTIVE MASS IN THREE DIMENSIONS

In this section we will outline the GW format for calculating the self-energy, and present numerical results for the 3D electron gas. It is well known that in 3D the effective mass ratio m^*/m is less than unity in the high-density limit. The high-density expansion ($r_s \ll 1$) was obtained in Refs. 2 and 3. In the metallic region ($1<r_s<8$) there has been some controversy about the behavior of the effective-mass ratio as a function of the ground-state density. The formalism for evaluating the self-energy part was put forward by Hedin[4] (GW approximation). In a more rigorous formulation[5] it can be summarized as follows. The standard starting point is the Dyson equation for the Green's function:

$$G_\sigma(\mathbf{k},\omega)=\frac{1}{\omega-\varepsilon_{\mathbf{k}}^{(0)}-\Sigma_\sigma(\mathbf{k},\omega)}, \tag{1}$$

with $\varepsilon_{\mathbf{k}}^{(0)}$ the unperturbed energy and $\Sigma_\sigma(\mathbf{k},\omega)$ the irreducible self-energy. The effective mass characterizes the quasiparticle excitation spectrum,

$$\varepsilon_{\mathbf{k}}=\frac{\mathbf{k}^2}{2m^*}, \tag{2}$$

and in terms of the self-energy is then given as

$$m^*/m=\left(1-\left.\frac{\partial\Sigma_\sigma(\mathbf{k},\omega)}{\partial\omega}\right|_{k=k_F}\right)\left(1+\frac{m}{k}\left.\frac{\partial\Sigma_\sigma(\mathbf{k},\omega)}{\partial k}\right|_{k=k_F}\right)^{-1}, \tag{3}$$

where m is the unrenormalized (bare) electron mass. The irreducible self-energy can be approximately expressed in Dyson equation form as

$$\Sigma_\sigma(\mathbf{k},\omega)=i\int\frac{d\mathbf{q}}{(2\pi)^3}\int\frac{d\omega'}{2\pi}W(\mathbf{q},\omega')G_\sigma(\mathbf{k}-\mathbf{q},\omega-\omega'), \tag{4}$$

where the W function incorporates the many-body effects. In general, it can be approximated by

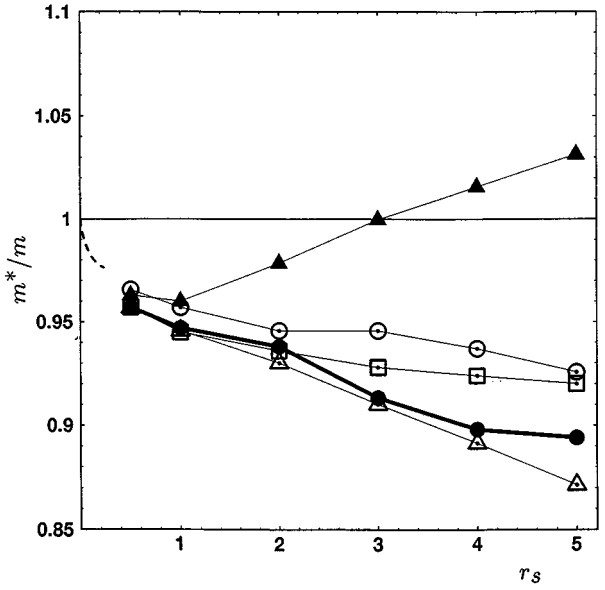

FIG. 1. The effective-mass ratio m^*/m vs the Seitz radius r_s for the 3D electron gas. Results of Hedin (Ref. 4) (solid triangles), Nakano and Ichimaru (Ref. 13) (empty circles), Yasuhara and Ousaka (Ref. 8) (empty squares), present (dark circles), and Rietschel and Sham (Ref. 7) (empty triangles). The dashed line is the high-density limit (Refs. 2 and 3). Our results indicate that the effective mass is a monotonically decreasing function of r_s throughout the whole metallic domain.

$$W(q,\omega)=\frac{v_q}{\epsilon(q,\omega)}\Gamma(q,\omega). \tag{5}$$

Here $v_q=4\pi e^2/q^2$ is the (3D) bare Coulomb interaction, $\epsilon(q,\omega)$ is the exact dielectric function, and $\Gamma(q,\omega)$ is the vertex correction.[6] In the work of Hedin[4] the random phase approximation (RPA) was adopted by putting $\Gamma=1$ and using the RPA dielectric response in (5):

$$W^{\mathrm{RPA}}(q,\omega)=v_k/\epsilon^{\mathrm{RPA}}(q,\omega). \tag{6}$$

Thus, the W function was just an effective RPA screened interaction. The self-energy was obtained by substituting the W function (6) into (4) and using the noninteracting Green's function in the right-hand side of (4). Results of Hedin are shown in Fig. 1 (solid triangles). The effective-mass ratio assumes its minimum at $r_s\approx 1$, then increases in the metallic region, and becomes greater than 1 for $r_s>3$. More recent results indicate a totally different behavior. In the self-consistent approach of Rietschel and Sham[7] the effective interaction function had the same form as in (6), but Eqs. (1) and (4) were solved self-consistently. Their results (Fig. 1, empty triangles) indicate that the effective-mass ratio is a monotonically decreasing function of r_s in the whole metallic domain. Similar results were obtained by Yasuhara and Ousaka[8] (Fig. 1, empty squares), who analyzed the Landau interaction function[9] using analytic fits based on the Monte Carlo results of Ceperly and Alder.[10] In their work the decrease in the quasiparticle mass was due to both spin-parallel and spin-antiparallel parts on the Landau interaction function. Another analysis of Landau interaction function based on Singwi, Sjölander, Tosi, and Land[11] was carried out in Ref. 12. Finally, a self-consistent scheme of Nakano and Ichimaru with the W function incorporating vertex correction (5) produced a similar decreasing behavior of the effective-mass ratio (Fig. 1, circles). Their procedure is rather involved; we refer to Ref. 13 for the details.

Our vehicle will now be the Sjölander-Stott (SS) theory of the two-component plasma.[1] As was recently shown,[14] it is essentially a fluid description of the electron gas, and does not directly employ the microscopic structure of the Fermi-liquid theory. It uses the correct linear response of the electron gas as an empirical input information. It is well known that this theory is capable of producing reliable density profiles around a repulsive impurity. The density profile equation resulting from the SS theory is

$$n_q^{\mathrm{ind,\,3D}}=f^{\mathrm{3D}}(q)\left[\,1+\frac{3}{4}\int_0^\infty k^2dk\left(\,1+\frac{q^2-k^2}{2qk}\ln\left|\frac{k+q}{k-q}\right|\right)\right.$$
$$\left.\times\, n_k^{\mathrm{ind,\,3D}}\right]. \tag{7}$$

This gives the induced electron density n_q^{ind} around an impurity of charge Z. Here, $f^{\mathrm{3D}}(q)$ is the induced electron density in the linear response approximation:

$$f^{\mathrm{3D}}(q)=\chi^{\mathrm{3D}}(q)\frac{4\pi Ze^2}{k_F^2q^2}.$$

The static linear response $\chi^{\mathrm{3D}}(q)$ is an input information and in our calculations was taken from the parametrization in Ref. 15. k,q are in units of the Fermi radius $k_F=(3\pi^2n)^{1/3}$, n being the homogeneous ground-state density. This profile relation has the correct high-q dependence, which is responsible for satisfying the cusp condition at the Coulomb source:

$$n_q^{\mathrm{ind,\,3D}}\big|_{q\to\infty}=Z\frac{16\lambda r_s}{3\pi q^3}\left(1+\frac{n^{\mathrm{ind,\,3D}}(\mathbf{r}=0)}{n}\right). \tag{8}$$

The major shortcoming of the profile relation (7) in the domain of repulsive impurities is overscreening by a hole. If the (repulsive) impurity charge is big enough the total electron density at the location of the impurity goes negative. For most of the possible physical applications this feature has an insignificant effect[16] because the region of the nonphysical behavior is very small and one can simply put the total electron density to 0 in this region. However, to be on the safe side, we restrict ourselves to the range of small enough impurity charges:

$$-0.3<Z^{\mathrm{3D}}<-0.03, \tag{9}$$

where the overscreening by a hole does not occur and one obtains a reliable density profile. We extract the effective single-particle scattering potential using the SS theory.[1,16] With this scattering potential we check the Friedel sum rule.

The Friedel sum rule is a condition on the difference of the trace of the logarithm of the single-particle scattering matrix between the top and the bottom of the band.[17,18] In our case of the jellium model of electron gas it takes a familiar form

$$Z=\frac{2}{\pi}\sum_{l=0}^{\infty} n_l \delta_l(k_F). \tag{10}$$

where the factor n_l accounts for the angular degeneracy:

$$n_l=\begin{cases} 2l+1 & \text{for 3D} \\ 2-\delta_{l,0} & \text{for 2D.} \end{cases}$$

The factor of 2 comes from the spin degeneracy, $\delta_l(k_F)$ are the partial wave scattering phase shifts at the Fermi momentum. This sum rule has been routinely used to adjust free parameters of the effective potential in a self-consistent fashion. In our case we take the effective potential from the SS theory.[1,16] With this effective potential we run a scattering calculation at the Fermi surface, and, having obtained the phase shifts $\delta_l(k_F)$, check the sum rule (10). The particles that are scattered at the Fermi surface are quasiparticles, not bare electrons. Their mass comes explicitly into the scattering calculation. We adjust this effective electron mass in the scattering calculation until (10) is satisfied within 0.01% accuracy. This provides us with the value for the effective mass. The procedure above is repeated for several values of Z from the region (9) in order to ensure that the results are independent of the impurity charge within a reasonable range

Our data for 3D are plotted on Fig. 1 (solid circles). They clearly indicate that the effective-mass ratio is a monotonously decreasing function of the Seitz radius throughout the whole metallic domain. In the high-density limit they (as well as all the other data) converge to the limiting behavior.[2,3] The agreement of our results with the most recent 3D calculations suggests that the same procedure can be tried in 2D since, in principle, the hydrodynamic model does not distinguish between dimensions as long as the correct linear response is employed. Now, we will consider the situation in two dimensions.

III. EFFECTIVE MASS IN TWO DIMENSIONS

Two-dimensional calculations based on the many-body formalism have been carried out within the same format of GW approximation. In the work of Jang and Min[19] the W function (5) is defined so that the vertex correction $\Gamma=1$. The dielectric function is expressed in a standard way in terms of the local field correction $\mathcal{G}(q,\omega)$:

$$\epsilon(q,\omega)=1-\frac{v_q\chi_0(q,\omega)}{1+v_q\mathcal{G}(q,\omega)\chi_0(q,\omega)}. \tag{11}$$

The notation here is as before, but refers to the 2D quantities: $v_q=2\pi^2/q$, and the noninteracting response $\chi_0(q,\omega)$ is as in Ref. 20. A further approximation is conventionally made that consists of replacing the dynamical local field correction by a frequency-independent one: $\mathcal{G}(q,\omega)=\mathcal{G}(q)$. Jang and Min employed different parametrizations for the $\mathcal{G}(q)$ together with the noninteracting Green's function in (4). Their approach was not self-consistent. The employed approximations were as follows: the RPA with $\mathcal{G}=0$; the Hubbard approximation (HA) adopted to the 2D by Jonson[21] with

$$\mathcal{G}^{\mathrm{HA}}(q)=\frac{1}{2}\frac{q}{\sqrt{q^2+k_F^2}}, \tag{12}$$

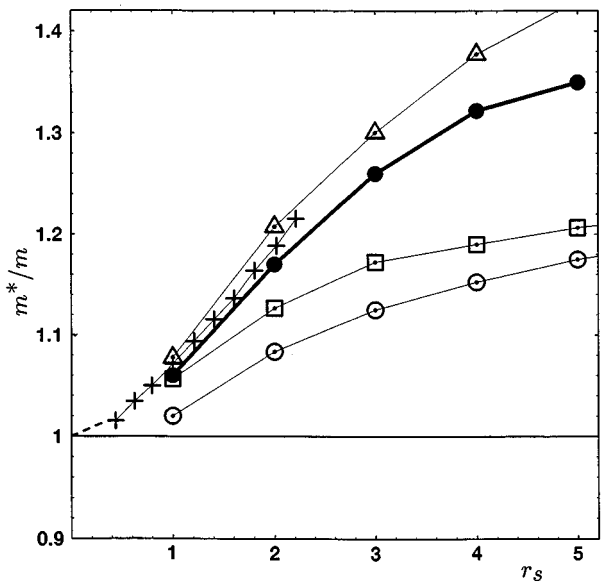

FIG. 2. The same as in Fig. 1. Results of Jang and Min (Ref. 19) in the Hubbard approximation (empty triangles), modified Hubbard approximation (empty boxes), RPA (empty circles), present theory (solid circles), and experimental data of Smith and Stiles (Ref. 25) (crosses). The dashed line is the high-density result (18) of Isihara and Toyoda (Ref. 26).

where $k_F=\sqrt{2\pi n}$ is the 2D Fermi radius; and the modified Hubbard approximation[22] (MHA) with

$$\mathcal{G}^{\mathrm{MHA}}(q)=\frac{1}{2}\sqrt{q^2+k_{\mathrm{F}}^2+k_{\mathrm{TF}}^2}, \tag{13}$$

where the Thomas-Fermi momentum is given by $k_{\mathrm{TF}}=2\pi ne^2/\varepsilon_F=\sqrt{2}r_s k_F$. The 2D Seitz radius is given by $\pi(r_s a_0)^2=1/n$. The effective-mass ratios produced by these approximations are plotted in Fig. 2: Hubbard approximation (empty triangles), modified Hubbard approximation (empty squares), and RPA (empty circles).

We proceed with the scheme we developed for the 3D case, but adapted to 2D. The profile relation coming from the Sjölander-Stott theory takes the form

$$n_q^{\mathrm{ind,\,2D}}=f^{\mathrm{2D}}(q)\left(1+\int_0^\infty kdk\,\frac{\Phi(q,k)}{\sqrt{k^2+q^2}}n_k^{\mathrm{ind,\,2D}}\right), \tag{14}$$

where the notation is the same as in (7), but refers to 2D. $\Phi(q,k)$ results from the angular integration:[23]

$$\Phi(q,k)=\frac{q}{\pi}\left(\frac{K[-2a_{q,k}/(1-a_{q,k})]}{\sqrt{1-a_{q,k}}}+\frac{K[2a_{q,k}/(1+a_{q,k})]}{\sqrt{1+a_{q,k}}}\right)-\frac{a_{q,k}k}{4}{}_2F_1\left(\frac{3}{4},\frac{5}{4},2,a_{q,k}^2\right), \tag{15}$$

with $a_{q,k}=2qk/k^2+q^2$. Here, $K(x)$ and ${}_2F_1(x)$ are the

complete elliptic integral of the first kind and the hypergeometric function, respectively. The induced density in the linear response approximation $f^{2D}(q)$ is taken from the parametrization[16] of the numerical results of Neilson *et al.*[24] Just like (7), (14) has the correct high-q dependence that is responsible for satisfying the cusp condition at the Coulomb source:

$$n_q^{\text{ind, 2D}}\big|_{q\to\infty} = \frac{Z\,2\sqrt{2}r_s}{q^3}\left(1+\frac{n^{\text{ind, 2D}}(\mathbf{r}=0)}{n}\right). \tag{16}$$

In order to avoid dealing with the overscreening by a hole we take the repulsive impurity charge to be small enough:

$$-0.1<Z^{2D}<-0.01. \tag{17}$$

As in the previous section, we extract the effective potential using the SS theory and run a 2D scattering calculation at the Fermi momentum adjusting the effective electron mass until the Friedel sum rule (10) is satisfied. Just as in 3D, we repeat the calculation for different values of Z within the range (17). Our results for the effective-mass ratio are shown in Fig. 2. They fit roughly in between the results of the HA and the MHA. The HA is known to take into account the exchange interaction and neglect correlations, while the MHA is an attempt to incorporate correlations. To compare with the experimental data we plot the magnetoconductivity measurements of Smith and Stiles[25] (Fig. 2, crosses). The agreement of our results with the experimental values is rather reasonable. We also plot the high-density expansion (Fig. 2, dashed line) obtained by Isihara and Toyoda[26] from the specific-heat calculation:

$$m^*/m = 1+0.043r_s. \tag{18}$$

This result was obtained by including first- and second-order exchange, as well as the ring diagram contributions for small but finite temperatures.

Finally, a few words about our numerical procedure would be appropriate. In the solution of (7) and (14) we could use (8) and (16), respectively, to approximate the high-q behavior, and after solving in the remaining domain match the solutions. This procedure is, however, very tedious and ineffective. We found that the solution is not affected if we solve the integral equation on the whole semi-infinite domain $[0,\infty)$ using the Gauss-rational rule for discretizing the integral. Of course, 2D calculations require care because of weaker convergence of integrals. In the scattering calculation we used twelve partial waves.

IV. CONCLUSION

We have presented our results for the electron effective-mass ratio using the effective potential coming from the SS theory for two and three dimensions. The calculations were carried out for small repulsive impurities where the SS works. The effective mass was extracted by enforcing the Friedel sum rule in the scattering calculation for the effective potential. We compared our results with the most recent numerical, as well as experimental data.

As for the 3D results (Fig. 1), there has been some uncertainty in the behavior of m^*/m in the metallic domain. Earlier results predicted that this ratio should increase with r_s, while more recent results indicate that it is a decreasing function of r_s. In our treatment the effective-mass ratio is a monotonically decreasing function of the Seitz radius in the whole metallic domain.

In 2D (Fig. 2) we present our results together with the results based on the GW approximation. Our treatment seems to fall ''in between'' the Hubbard and the modified Hubbard approximations. Our results give reasonable agreement with the experimental data.

In conclusion, it is interesting to relate the 2D and 3D results between themselves. It is well known that the exchange interaction diminishes the effective mass, while correlations shift it in the opposite direction. The quasiparticle effective mass is a result of an interplay between the exchange and correlation contributions. It comes as no surprise that because correlations are stronger in 2D than in 3D, generally, the effective mass is greater in 2D than in 3D for the same value of r_s.

ACKNOWLEDGMENTS

The authors would like to thank Professor I. Nagy for providing some of the most important references for this work and Professor J. L. Birman for extremely helpful discussions. Partial support of the National Science Foundation and the Physics Department at New York University is gratefully acknowledged.

[1] A. Sjölander and M. S. Stott, Phys. Rev. B **5**, 2109 (1972).
[2] M. Gell-Mann, Phys. Rev. **106**, 369 (1957).
[3] D. F. DuBois, Ann. Phys. **7**, 174 (1959).
[4] L. Hedin, Phys. Rev. **139**, A796 (1965).
[5] S. Ichimaru, *Statistical Plasma Physics* (Addison-Wesley, New York, 1994).
[6] A. Nakano and S. Ichimaru, in *Strongly Coupled Plasma Physics*, edited by by S. Ichimaru (North-Holland/Yamada Science Foundation, Amsterdam, 1990).
[7] H. Rietschel and L. J. Sham, Phys. Rev. B **28**, 5100 (1983).
[8] H. Yasuhara and Y. Ousaka, Solid State Commun. **64**, 673 (1987).
[9] P. Noziéres, *The Theory of Interacting Fermi Systems* (Benjamin, New York, 1969).
[10] D. M. Ceperly and B. J. Alder, Phys. Rev. Lett. **45**, 566 (1980).
[11] K. S. Singwi, A. Sjölander, M. P. Tosi, and R. H. Land, Phys. Rev. B **1**, 1044 (1970).
[12] G. Pizzimenti, M. P. Tosi, and A. Villari, Lett. Nuovo Cimento **2**, 81 (1971).
[13] A. Nakano and S. Ichimaru, Phys. Rev. B **39**, 4930 (1989); **39**, 4938 (1989).
[14] A. Krakovsky and J. K. Percus, Phys. Rev. B **52**, 7901 (1995).
[15] B. Farid, V. Heine, G. E. Engel, and I. J. Robertson, Phys. Rev. B **48**, 11 602 (1993).
[16] A. Krakovsky and J. K. Percus, Phys. Rev. B **52**, R2305 (1995).
[17] J. Friedel, Philos. Mag. **43**, 153 (1952).
[18] J. S. Langer and V. Ambegaokar, Phys. Rev. **121**, 1090 (1961).

[19] Y.-R. Jang and B. I. Min, Phys. Rev. B **48**, 1914 (1993).
[20] F. Stern, Phys. Rev. Lett. **18**, 546 (1967).
[21] M. Jonson, J. Phys. C **9**, 3055 (1965).
[22] T. M. Rice, Ann. Phys. (N.Y.) **31**, 100 (1965).
[23] We used MATHEMATICA 2.1 symbolic integration packages.
[24] D. Neilson, L. Świerkowski, A. Sjölander, and J. Szymański, Phys. Rev. B **44**, 6291 (1991).
[25] J. L. Smith and P. J. Stiles, Phys. Rev. Lett. **29**, 102 (1972).
[26] A. Isihara and T. Toyoda, Phys. Rev. B **21**, 3358 (1980).